Published in final edited form as:
Science. 2008 September 5; 321(5894): 1322–1327. doi:10.1126/science.1159775.

Internally Generated Cell Assembly Sequences in the Rat Hippocampus

Eva Pastalkova[1], **Vladimir Itskov**[1,2], **Asohan Amarasingham**[1], and **György Buzsáki**[1,*]

1*Center for Molecular and Behavioral Neuroscience, Rutgers, The State University of New Jersey, 197 University Avenue, Newark, 07102 New Jersey, U. S. A.*

Abstract

A longstanding conjecture in neuroscience is that aspects of cognition depend on the brain's ability to self-generate sequential neuronal activity. We found that reliably and continually-changing cell assemblies in the rat hippocampus appeared not only during spatial navigation but also in the absence of changing environmental or body-derived inputs. During the delay period of a memory task each moment in time was characterized by the activity of a unique assembly of neurons. Identical initial conditions triggered a similar assembly sequence, whereas different conditions gave rise, uniquely, to different sequences, thereby predicting behavioral choices, including errors. Such sequences were not formed in control, non-memory, tasks. We hypothesize that neuronal representations, evolved for encoding distance in spatial navigation, also support episodic recall and the planning of action sequences.

A prominent theory states that the hippocampal system primarily serves spatial navigation (1,2), a component of which is that the place-dependent activity of neurons ("place cells"; 1, 2) in the hippocampus arises from external, serially ordered environmental stimuli (3-7). Place cells are thought to embody the representation of a 'cognitive map', enabling flexible navigation. However, neural theories of other cognitive processes that may depend on the hippocampus, such as episodic memory and action planning, draw upon the activity of hypothetical, internally organized "cell assemblies" (8-13).

Several observations refine the navigation theory. Hippocampal neurons can predict where the animal is coming from, or its destination (14-17); the sequential activity of place cells during locomotion is replicated within single cycles of the theta oscillation (8-12 Hz; 18-20); furthermore, the temporal recruitment of active neurons in the population bursts of rest and sleep also reflects, again on a faster time scale, their sequential activity as place cells, during locomotion (21-23). Thus, the sequential activation of hippocampal neurons can be disengaged from external landmarks (24-25). However, internally-generated assembly sequences operating at the time scale of behavior have not yet been reported.

The frameworks of environment-controlled versus internally-generated assembly sequences give rise to distinct predictions. Imagine that a rat is 'frozen' in position during its travel (and yet, importantly, the theta oscillation is maintained). According to the navigation theory, a subset of landmark-controlled place cells should then display sustained activity, and other neurons would remain suppressed (2-6). In contrast, if assembly sequences were generated by internal mechanisms, neurons might rather display continually-changing activity. We tested these predictions by examining the activity of hippocampal neurons while the rat was required

[2]Present address: Center for Neurobiology and Behavior, Columbia University, 1051 Riverside Drive, New York, NY 10032
[*]To whom correspondence should be addressed: E-mail: buzsaki@axon.rutgers.edu

to run in a wheel at a relatively constant speed (26-27), during the delay of a hippocampus-dependent alternation memory task.

Internally generated cell assembly sequences

Rats were trained to alternate between the left and right arms of a figure-8 maze (Fig. 1A; Supporting Online Material). During the delay period between maze runs (10 sec for rat 1; 20 sec for rats 2 and 3), the animals were trained to run steadily in the same direction in a wheel (Fig. 1A). To confront the predictions of the navigation theory with those of the internal sequence generation hypothesis, we compared the firing patterns of CA1 hippocampal neurons in the wheel and the maze.

We analyzed the activity of ~500 pyramidal cells in the wheel and ~600 neurons in the maze (Fig. 1A; mean firing rate > 0.5Hz). Pyramidal neurons were transiently active in both the maze (place cells; 1), and the wheel. Although the position and direction of the rat's head was stationary during wheel running (fig. S1), the percentage of neurons active in the pixels occupied by the head during wheel running was 3 to 4 times higher than at any area of comparable size in the maze (Fig. 1B; Wilcoxon rank sum test: $p < 0.0001$). Thus, if pyramidal neurons were solely activated by environmental cues (2-6), this finding would reflect several-fold stronger neuronal representation of the animal's position within the wheel. Many individual pyramidal cells were active in both the wheel and the maze but the sequential order of their activation in the wheel was unrelated to that in the maze, and their firing rates in these two areas were inversely correlated (Figs. 1C; 4B, $r_s = -0.3$, $p < 0.0001$, $n = 681$; in contrast to the population of interneurons, fig. S2; $r_s = 0.85$; $p < 0.0001$, $n = 125$). The average proportion of pyramidal neurons simultaneously active (i.e., firing at least a single spike in 100-msec windows, and averaging over 100-msec windows) was similar in the wheel (10.75 ± 3.97%) and the maze (12.56 ± 4.32%; fig. S3).

Pyramidal neurons typically fired transiently, and reliably in successive trials, at specific times of wheel running ('episode fields'), and most cells had multiple peaks of varying sizes (Fig. 1D). Typically, and reminiscent of a 'synfire chain' (11), at least one episode cell was active at every moment of a wheel run (Fig. 1E).

Were episode cells in the wheel generated by the same mechanism as place cells in the maze? We looked for evidence for differing mechanisms by comparing several measures of the firing of episode and place cells. First, we calculated the duration of activity (field width; Fig. 1F) of single cells (including only fields with a peak firing rate ≥6.0 Hz and ≥4.5 SD above the mean firing rate; S.O.M). The temporal (or spatial) extent of the field was determined as those times (positions) with firing rates at least 10% that of the peak firing rate (in the wheel or maze) (19,28). By these criteria, 32 % of the neurons in the wheel and 22% in the maze had at least one field. Neither the distribution of field widths (medians: 0.94 sec and 1.0 sec, respectively, $p = 0.44$; Wilcoxon test) nor peak firing rates (medians: 13.08 Hz; and 12.8 Hz, respectively; $p = 0.61$) differed significantly between episode and place fields (Fig. 1F). Second, to measure the average 'lifetime' of assembly activity for a population, we determined the maximal time lag at which the auto-correlation of the population's activity was above 0.5 (29), and again found no significant difference, with respect to the median, between the populations of episode and place cells (Fig. 1G; medians: 0.83 sec and 0.75sec, respectively, $p = 0.32$). Third, we compared the relationship between spikes and the local field potential. On linear tracks, sequentially generated spikes of a place cell gradually shift to earlier and earlier phases of the theta oscillation as the rat passes through the place field ("phase precession"), and there is a systematic relationship between the phase of spikes and the animal's position (3,18-20,28, 30-31). The navigation theory predicts that the phase of spikes will remain fixed if environmental inputs do not change (3,26-27). In contrast, episode cells displayed phase

precession during wheel running (Fig. 2A). Similarly to place cells, the theta frequency oscillation of episode cells was higher than that of the field theta rhythm (Fig. 2B), and the slope of phase precession was inversely related to the length of the episode field (Fig. 2A, 2D; 3,19,20,28,30-31). Furthermore, the slopes correlated more strongly with the length of the episode field ($r_s = 0.52$, $p < 0.0001$) than with the time it took the rat to run through the same field ($r_s = 0.46$, $p < 0.0001$) (Fig. 2D;3), due to the variability of the rat's running speed (28). Importantly, the distributions of phase precession slopes for the episode and place fields were also similar (Fig. 2C; medians, −0.6 deg/sec and −0.6 deg/sec, respectively $p = 0.6$). Finally, we compared the spike timing relationships among neurons. During maze traversals, the distance between the place field peaks of a neuronal pair is correlated with the temporal offset between its spikes within the theta cycle, a phenomenon known as distance-time 'compression' (18,19; S.O.M.). Analogously, the distance between peaks of the episode fields of neuron pairs (episode fields with peak firing rate > 5Hz and > 3SD above the mean firing rate were included in this analysis; n = 105 pairs) was correlated with the temporal offsets between the spikes at the theta time scale (Fig. 2E, $r_s = 0.59$, $p < 0.0001$). These findings indicate that the mechanisms generating place and episode fields are similar.

Body cues are not sufficient to generate assembly sequences

It has been suggested that in addition to generating a cognitive map of the environment (2), the hippocampus and its associated structures integrate self motion-induced information (7, 32-33). Were the episode cell sequences generated by 'idiothetic', self-motion cues? We examined population firing patterns in two, non-memory, control tasks. In the first task (control 1), the animals (rats 3 and 4) were required to run in the wheel for water reward available in an adjacent box (26). In the second task (control 2), the animals (rats 2 and 3) had continuous access to a wheel adjacent to their home cage, and recordings were made during 'spontaneous' wheel running episodes. Transient firing patterns, consistent across trials, were rarely observed in the control tasks. Rather, the majority of active neurons exhibited relatively sustained firing throughout the wheel-running periods (Fig. 3A;fig. S4, 5;26-27). During runs of opposite direction in the wheel, different populations of neurons were active (fig. S5;26), arguing for the importance of distant cues (2,20), and against a critical role of idiothetic inputs (26). In addition, the temporal organization of cell assemblies in control tasks was less precise, as reflected by much weaker correlations between temporally-adjacent populations in the control than in the memory task (Fig. 3B,C), and despite the similarity in firing rates in all tasks (fig. S6). As another contrast to the memory task, neurons in the control tasks fired throughout the trial with spikes locked to a similar phase of the theta cycle (Fig. 3A). Consistent with these observations, neurons in the memory task oscillated faster than the LFP ($\Delta = 0.44 \pm 0.6$ Hz; Figs. 2B,3D,E), an indication of phase precession (19,20,29,30), whereas in the control tasks the power spectra of the units and LFP were similar ($\Delta = 0.07 \pm 0.3$ Hz; Fig. 3E). Finally, to quantify differences in temporal clustering of spikes, we examined an autocorrelogram of each neuron. We applied (after filtering; 0.2-2 Hz) the same definition of the boundary of the episode field (i.e., the '10% boundary') and then compared, for each neuron, the ratio of the number of spikes that fell within the boundary to those that fell outside. These ratios were significantly larger in the memory task, and reflected the temporal compactness of firing in the memory, as opposed to the control, tasks (Fig. 3F). Thus, the indicators of temporally-precise sequential activity in neuronal populations were absent in the control tasks, despite indistinguishable motor characteristics across all tasks.

Assembly sequences depend on memory load

What is the behavioral significance of internally generated cell assembly sequences? Temporarily inactivating neuronal circuits in the dorsal hippocampus, we found that performance in the delayed alternation task depends on the integrity of the hippocampus (fig.

S7; 17). Thus, we hypothesized that information about choice behavior is reflected in assembly sequences (34). All correctly-performed trials were sorted according to the rat's future choice of arm (i.e., left or right), and choice-specific firing effects were identified by comparing the firing patterns of single neurons with those of surrogate spike trains created by shuffling the left and right labels (Fig. 4A, B;34; S.O.M.). Some neurons were active exclusively before either the left or right choice, others showed differential firing rates and/or fired at different times after the beginning of wheel running (Fig. 4A; fig. S8, S9, S10; movie 1). The largest proportion of neurons exhibiting choice-predictive activity was at the beginning of the run; this proportion decreased as a function of time during the delay and in the stem of the maze (Fig. 4B), suggesting a critical role for initial conditions in specifying the sequences (fig. S11). In addition, we designed a probabilistic model of the relationship between neuronal firing patterns and the animal's choices (S.O.M.). Using this model, the accuracy of single-trial prediction, under cross-validation, varied from low (near 50%) and not significant, to 100% and significant, across many sessions (Fig. S9).

Because the rat was performing an alternation task, past and future choices were deterministically related on correctly-performed trials, and it was not possible to disambiguate their influence on neuronal activity. To distinguish such retrospective and prospective factors (14-17), we examined cell assembly sequences during error trials. Neurons which reliably predicted the behavioral choice of the rat on correct trials continued to predict the choice behavior on error trials (Fig. 5A;fig. S12;movie 1;15,24). Similarly, population sequences which differentiated correct behavioral choices continued to predict behavioral choice errors (Fig. 5B, C; fig. S13). Although there were only a few error trials, a majority of them could be predicted from the firing patterns of neurons during wheel running (Fig. 5D). Altogether, these observations demonstrate that a unique sequence of neurons was activated in a reliable temporal order from the moment the rat entered the wheel to the time it reached the reward.

Because running speed, head position and head direction during wheel running before left and right choices were apparently indistinguishable (fig. S1), the above findings indicate that trial differences in hippocampal assembly configurations cannot solely arise from instantaneous environmental inputs or the integration of motion signals.

Behavioral significance of internally generated cell assembly sequences

These findings demonstrate that the rat brain can generate continually-changing assembly sequences. The patterns of the self-evolving neuronal assembly sequences depend on the initial conditions and the unique sequences of cell assemblies are predictive of behavioral outcome.

Our results offer new insights on the relationship between hippocampal activity and navigation (2-7,14-20,26-30,33). Hippocampal firing patterns during maze navigation were similar to those during wheel running in the delayed alternation memory task with stationary environmental and body cues. Therefore, we suggest that hippocampal networks can produce sequential firing patterns in two, possibly interacting, ways: under the influence of environmental/idiothetic cues or by self-organized internal mechanisms. The high-dimensional and largely ‘random’ (i.e., non-topographical) connectivity of the CA3 axonal system (35) and its inputs makes the hippocampus an ideal candidate for internal sequence generation (13,33, 36-37). The parameters of cell assembly dynamics (including their trajectory and lifetimes) are likely affected by a number of factors, including experience-dependent and short-term synaptic plasticity (34,38), asymmetric inhibition (39), brain state, and fundamentally, the character and context of the input. The evolving trajectory can be effectively perturbed or ‘updated’ by external inputs in every theta cycle (40). Because of this flexibility in the sources of cell assembly control, we hypothesize that neuronal algorithms, having evolved for the computation of distances, can also support the episodic recall of events and the planning of

action sequences and goals (19). During learning, the temporal order of external events is instrumental in specifying and securing the appropriate neuronal representations, whereas during recall, imagination (35) or action planning the sequence identity is determined by the intrinsic dynamics of the network.

Supplementary Material

Refer to Web version on PubMed Central for supplementary material.

Acknowledgements

We thank H. Hirase for sharing his data, and C. Curto, C. Geisler, S. Ozen, S. Fujisawa, K. Mizuseki, A. Sirota and D. W. Sullivan and R. L. Wright for comments. Supported by NIH NS34994 and MH54671, NSF SBE0542013, James S. McDonnell Foundation, NSF (A. A.), The Swartz Foundation (V. I.), Robert Leet & Clara Guthrie Patterson Trust (E. P.).

References and Notes

1. O'Keefe J, Dostrovsky J. Brain Res 1971;34:171–175. [PubMed: 5124915]
2. O'Keefe, J.; Nadel, L. The hippocampus as a cognitive map. Clarendon Press; Oxford, UK: 1978.
3. Huxter J, Burgess N, O'Keefe J. Nature 2003;425:828–832. [PubMed: 14574410]
4. McNaughton BL, Barnes CA, O'Keefe J. Exp. Brain Res 1983;52:41–49. [PubMed: 6628596]
5. O'Keefe J, Burgess N. Nature 1996;381:425–8. [PubMed: 8632799]
6. Muller RU, Kubie JL, Ranck JB Jr. J. Neurosci 1987;7:1935–1950. [PubMed: 3612225]
7. McNaughton BL, Barnes CA, Gerrard JL, Gothard K, Jung MW, Knierim JJ, Kudrimoti H, Qin Y, Skaggs WE, Suster M, Weaver KL. J. Exp. Biol 1996;199:173–185. [PubMed: 8576689]
8. Hebb, DO. The Organization of Behavior: A Neuropsychological Theory. Wiley; New York: 1949.
9. Tulving, E. Elements of episodic memory. Clarendon Press; Oxford, England: 1983.
10. Squire LR. Psychol. Rev 1992;99:195–231. [PubMed: 1594723]
11. Abeles, M. Corticotronics: Neural Circuits of the Cerebral Cortex. Cambridge Univ. Press; New York: 1991.
12. Howard MW, Fotedar MS, Datey AV, Hasselmo ME. Psychol. Rev 2005;112:75–116. [PubMed: 15631589]
13. Levy WB, Hocking AB, Wu X. Neural Networks 2005;18:1242–1264. [PubMed: 16269237]
14. Frank LM, Brown EN, Wilson M. Neuron 2000;27:169–178. [PubMed: 10939340]
15. Ferbinteanu J, Shapiro ML. Neuron 2003;40:1227–1239. [PubMed: 14687555]
16. Wood ER, Dudchenko PA, Robitsek RJ, Eichenbaum H. Neuron 2000;27:623–633. [PubMed: 11055443]
17. Ainge JA, van der Meer MA, Langston RF, Wood ER. Hippocampus 2007;17:988–1002. [PubMed: 17554771]
18. Skaggs WE, McNaughton BL, Wilson MA, Barnes CA. Hippocampus 1996;6:149–172. [PubMed: 8797016]
19. Dragoi G, Buzsáki G. Neuron 2006;50:145–57. [PubMed: 16600862]
20. Huxter JR, Senior TJ, Allen K, Csicsvari J. Nature Neurosci 2008;11:587–94. [PubMed: 18425124]
21. Buzsáki G. Neuroscience 1989;31:551–570. [PubMed: 2687720]
22. Wilson MA, McNaughton BL. Science 1994;265:676–679. [PubMed: 8036517]
23. Louie K, Wilson MA. Neuron 2001;29:145–56. [PubMed: 11182087]
24. Deadwyler SA, Bunn T, Hampson RE. J. Neurosci 1996;16:354–72. [PubMed: 8613802]
25. Eichenbaum H, Dudchenko P, Wood E, Shapiro M, Tanila H. Neuron 1999;23:209–26. [PubMed: 10399928]
26. Czurko A, Hirase H, Csicsvari J, Buzsáki G. Eur. J. Neurosci 1999;11:344–352. [PubMed: 9987037]

27. Hirase H, Czurko A, Csicsvari J, Buzsáki G. Eur. J. Neurosci 1999;11:4373–4380. [PubMed: 10594664]
28. Geisler C, Robbe D, Zugaro M, Sirota A, Buzsáki G. Proc. Natl. Acad. Sci. U. S. A 2007;104:8149–54. [PubMed: 17470808]
29. Gothard KM, Skaggs WE, McNaughton BL. J. Neurosci 1996;16:8027–8040. [PubMed: 8987829]
30. O'Keefe J, Recce ML. Hippocampus 1993;3:317–330. [PubMed: 8353611]
31. Maurer AP, Cowen SL, Burke SN, Barnes CA, McNaughton BL. J. Neurosci 2006;26:13485–92. [PubMed: 17192431]
32. Sargolini F, Fyhn M, Hafting T, McNaughton BL, Witter MP, Moser MB, Moser EI. Science 2006;312:758–62. [PubMed: 16675704]
33. McNaughton BL, Battaglia FP, Jensen O, Moser EI, Moser MB. Nature Rev. Neurosci 2006;7:663–678. [PubMed: 16858394]
34. Fujisawa S, Amarasingham A, Harrison MT, Buzsáki G. Nature Neurosci 2008;11:823–833. [PubMed: 18516033]
35. Li XG, Somogyi P, Ylinen A, Buzsáki G. J. Comp. Neurol 1994;339:181–208. [PubMed: 8300905]
36. Kreiman G, Koch C, Fried I. Nature 2000;408:357–61. [PubMed: 11099042]
37. Lisman JE. Neuron 1999;22:233–242. [PubMed: 10069330]
38. Abbott LF, Regehr WG. Nature 2004;431:796–803. [PubMed: 15483601]
39. Rabinovich M, Huerta R, Laurent G. Science 2008;321:48–50. [PubMed: 18599763]
40. Zugaro MB, Monconduit L, Buzsáki G. Nat. Neurosci 2005;8:67–71. [PubMed: 15592464]

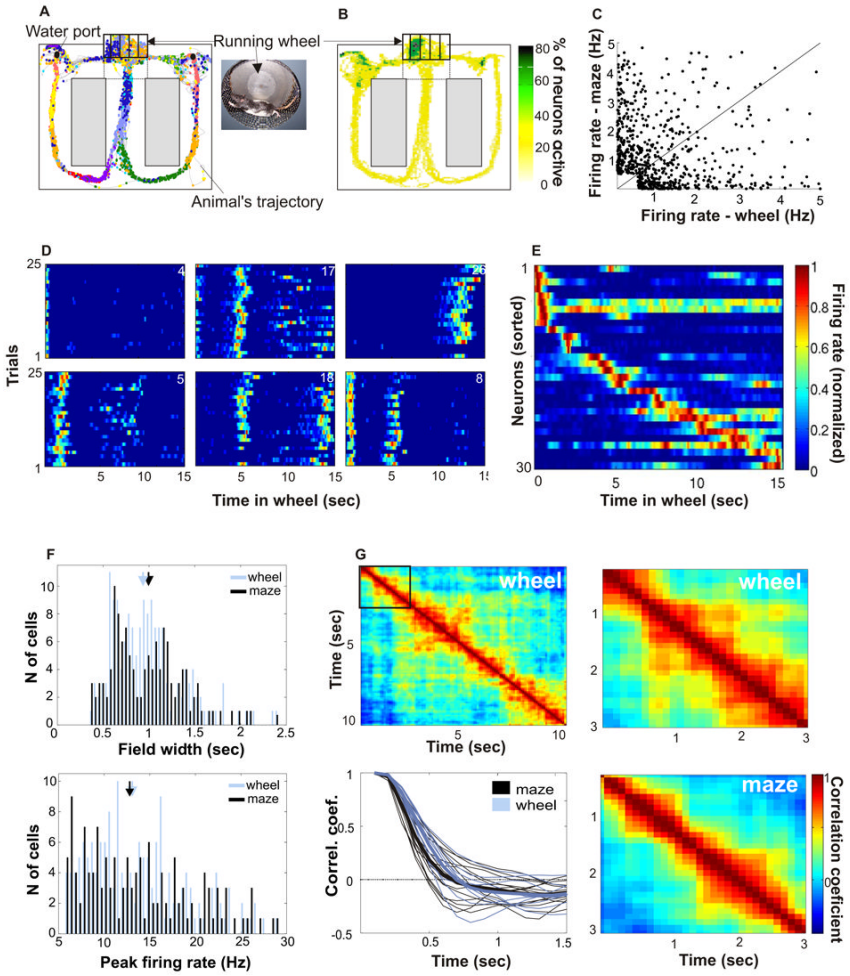

Fig. 1.

"Episode fields" in the wheel and place fields in the maze are similar. (**A**) Color-coded spikes (dots) of simultaneously recorded hippocampal CA1 pyramidal neurons. The rat was required to run in the wheel facing to the left during the delay between the runs in the maze. (**B**) Percent of neurons firing >0.2 Hz within each pixel. Note the highest percentage of active neurons in the wheel. (**C**) Relationship between firing rate of neurons in the wheel and the maze ($r_s = -0.3$, $p < 0{,}0001$, 681 neurons, 3 rats, 17 sessions). (**D**) Normalized firing rate of six simultaneously recorded neurons during wheel running (each line shows the color-coded activity on single trials turning to the left arm). Note the transient increase of firing rate ("episode fields") at specific segments of the run. (**E**) Normalized firing rate of 30 simultaneously recorded neurons during wheel running, ordered by the latency of their peak firing rate. (**F**) Width (top) and peak firing rate (bottom) of episode and place fields (N_{wheel}= 135, N_{maze}=162). Arrows: medians. G. Population vector cross-correlation matrix (S.O.M.). The width of the diagonal stripe indicates the rate at which neuronal assemblies transition. Lower left: decay of population vector correlation during wheel running and maze traversal. Thin lines: individual sessions; thick lines: group means.

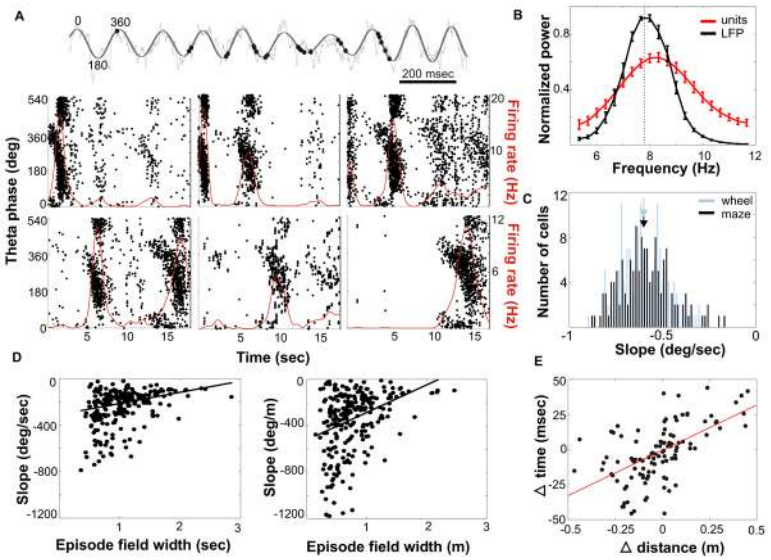

Fig. 2.

Episode neurons in the wheel display theta phase precession and 'temporal compression". (**A**) Top, unfiltered (gray) and filtered (4-10 Hz; black) traces of LFP and phase advancement of action potentials (dots). Below, activity of 6 example neurons from the same session. Each dot is an action potential, displayed as a function of theta phase and time from the beginning of wheel running from all trials. One and a half theta cycles are shown (y axis). Red line, smoothed firing rate. (**B**) Power spectra of spike trains generated during wheel running (n = 283 pyramidal neurons) and the simultaneously recorded LFP. Note faster oscillation of neurons relative to LFP. (**C**) Slope of theta phase precession within episode fields in the wheel and within place fields in the maze. (**D**) Relationship between phase precession slope and episode length (left, $r = 0.46$, $p < 0.0001$) and episode field width (right, $r = 0.52$, $p < 0.0001$), respectively. (**E**) Temporal "compression" of spikes sequences. Correlation of the distance between the peaks of episode fields of neuron pairs in the wheel with the temporal offset of the pair's cross-correlogram peak. Each dot represents a neuron pair (n = 105 eligible pairs; 3 rats; $r = 0.59$; $p < 0.0001$).

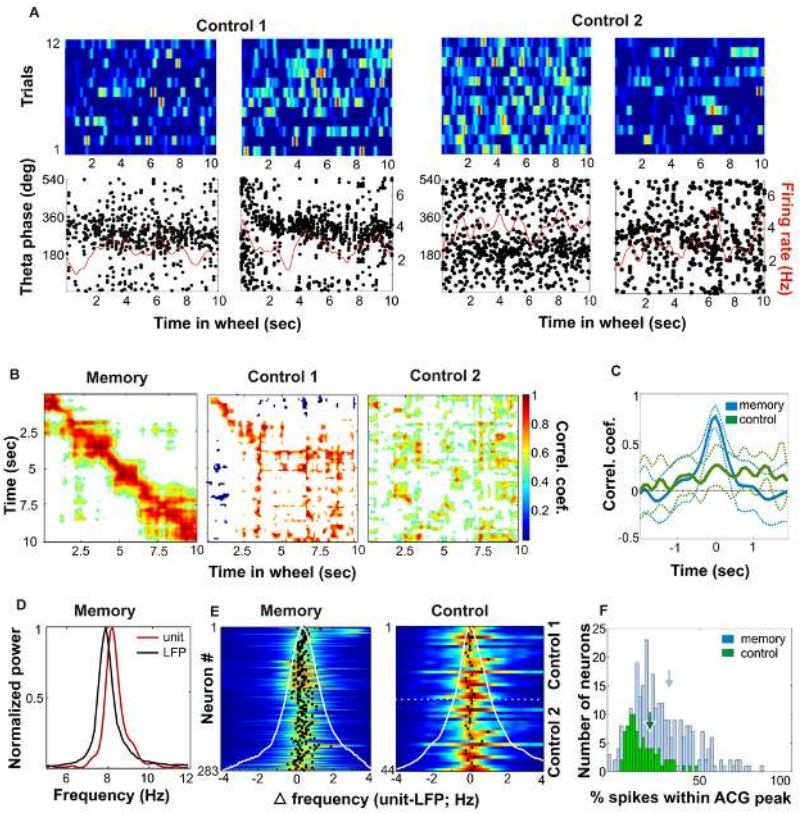

Fig. 3.

Firing patterns during wheel running depend on the context of the task. (**A**) Top, Activity of representative single neurons (color coded) during wheel running in control tasks 1 and 2 (compare with Fig. 1D). Bottom, unit discharges (dots) from all trials within a session as a function of theta phase, plotted against time from the beginning of a wheel run. Gray line, smoothed mean firing rate. Note relatively steady firing rates and steady theta phase in both control tasks. (**B**) Cross-correlation matrices in three different tasks (memory and control 2 are from the same rat). In the memory task, trials with the same future choices (L-trials$_n$ vs L-trial$_{n+1}$ and R-trials$_n$ vs R-trial$_{n+1}$) were cross-correlated, whereas in control tasks trials$_n$ and trials$_{n+1}$ were cross-correlated. Only pixel values significantly different from chance are shown (Spearman rank correlation, $p < 0.01$). (**C**) Population vector correlation coefficient values in the memory task (n = 17 sessions) and control tasks (n = 8 sessions). Mean ± SD. (**D**) Power spectrum of spike trains of an episode neuron (unit) and simultaneously recorded LFP during wheel running in the memory task (30). Note the higher frequency of unit firing oscillation, relative to the frequency of LFP. (**E**) Difference between unit and LFP oscillation frequency in the memory (left) and control (right) tasks. Each line is a color-coded normalized cross-correlogram between power spectrum of a pyramidal neuron and simultaneously recorded LFP. A shift of the maximal correlation values to the right indicates that unit theta oscillation is faster than LFP theta oscillation (black dots, maxima of the cross-correlograms; white line, sum of all neurons). Note significant frequency shift in the memory task (0.44 ± 0.6Hz), and lack of frequency shift in control tasks (combined control 1 and 2: 0.07 ± 0.3Hz) (**F**) Ratio of spikes in the center and tail of temporal auto-correlograms (S.O.M.). High values indicate compact episode fields, low values indicate spikes scattered throughout the time of wheel running (memory task, n=287 neurons; control tasks, n = 85 neurons $p < 0.0001$; ranksum test). Arrows, medians.

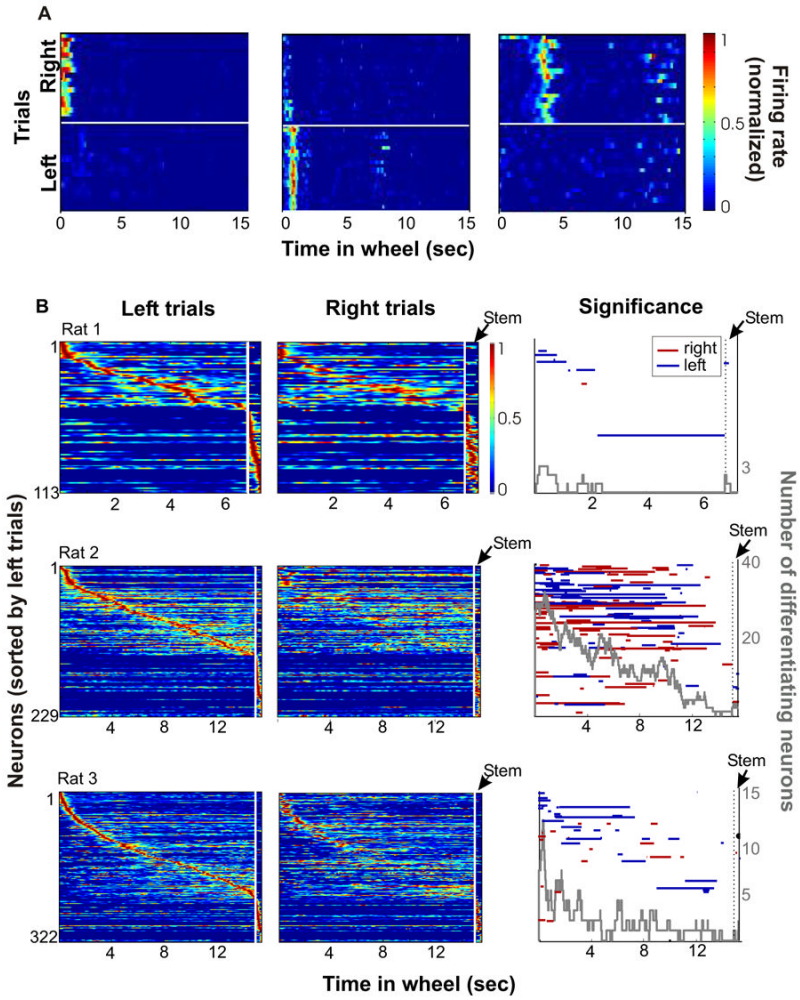

Fig. 4.

Cell assembly activity in the wheel predicts future choice of the rat in the maze. (**A**) Examples of 3 neurons which strongly differentiated between wheel running trials preceding right and left choices (see also fig. S7 and movie 1). (**B**) Normalized firing rate profiles of neurons during wheel running and in the stem of the maze, ordered by the latency of their peak firing rates during left trials (each line is a single cell; cells are combined from all sessions). White line, time gap between the end of wheel running and the initiation of maze stem traversal. Middle panel: Normalized firing rates of the same neurons during right trials. Right panel: Time periods of significant differences ($p < 0.05$) in firing rates between left and right trials for respective neurons (red line: R > L, blue line: L > R). Grey line, number of neurons discriminating between left and right trials as a function of wheel running time.

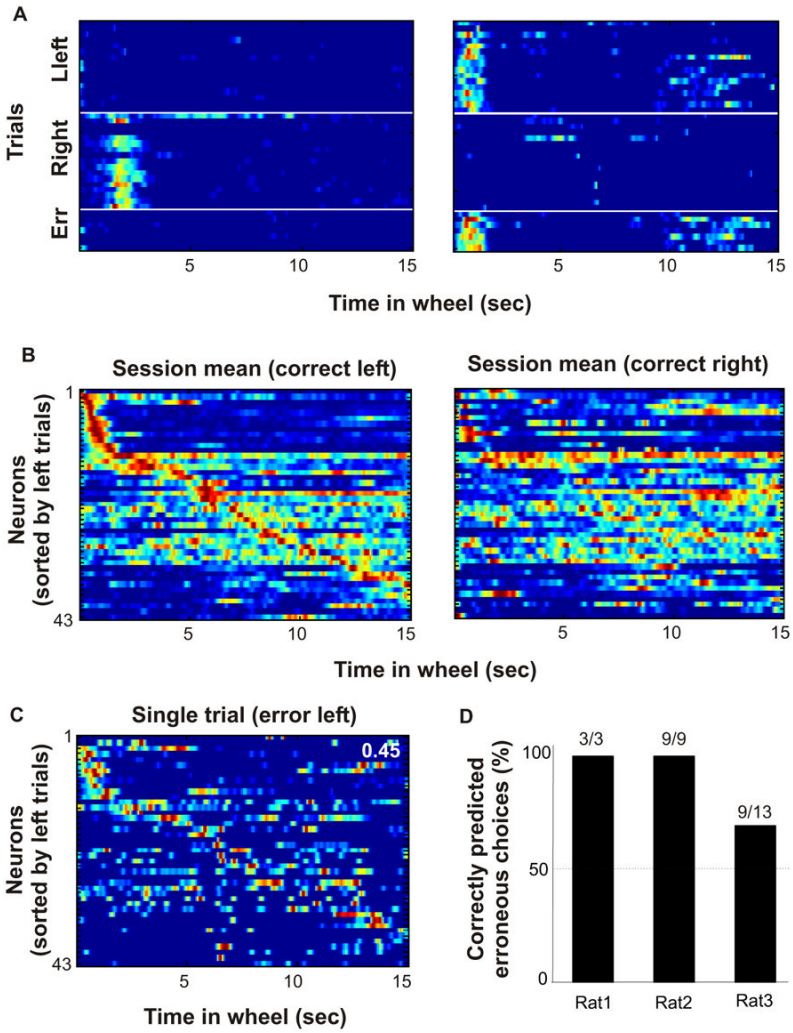

Fig. 5.

Cell assembly activity in the wheel predict behavioral errors in the maze. (**A**) Two example neurons from a session with 7 left error trials (err). Correct trials are separated to left and right turn trials. (**B**) Normalized firing rates of 43 neurons simultaneously recorded during wheel running, ordered by the latency of peak firing rates during correct left trials (left). Right, firing sequence of the same neurons on correct right trials. (**C**) Firing sequence of neurons in a single error (left) trial. Neuronal order is the same as in **B**. Note that the firing sequence during the error trial is similar to that of the correct left trials. White number: correlation coefficient between correct and error trial sequences (see also fig. S13). (**D**) Percent of correctly predicted errors from the neuronal population activity.